Kinetics of photorefractive recording for circular light beams

M. Kösters,[1] B. Sturman,[2] D. Haertle,[1] and K. Buse[1]

[1]Institute of Physics, University of Bonn, Wegelerstrasse 8, D-53115 Bonn, Germany
[2]Institute of Automation and Electrometry, Koptyug Avenue 1, 630090 Novosibirsk, Russia

Received December 3, 2008; revised February 17, 2009; accepted February 25, 2009; posted February 27, 2009 (Doc. ID 104661); published March 25, 2009

We show, theoretically and experimentally, that the buildup of the space-charge field in photorefractive crystals is far from monoexponential for circular light beams. This is a general property of the two-dimensional (2D) case, in contrast to the one-dimensional case. The results form a basis for determination of the photoelectric parameters of photorefractive crystals within a wide intensity range, which is important, e.g., for solving of the optical-damage problem in $LiNbO_3$ and $LiTaO_3$ crystals. © 2009 Optical Society of America

OCIS codes: 090.2900, 090.7330, 120.4630.

It is widely accepted that the buildup and relaxation of space-charge fields in photorefractive crystals obey a single-exponential law [1–3]. The corresponding rate constant is expected to be the inverse dielectric relaxation time when the characteristic spatial size of the light pattern is not too small. This premise has its roots in considerations of one-dimensional (1D) cases—recording of plane index gratings and 1D strips. A single-exponential fit to experimental kinetic curves traditionally serves for determination of the charge transport properties [1–3]. Rare deviations from the single-exponential law indicate the presence of two (or more) microscopic buildup/relaxation mechanisms.

Two-dimensional (2D) configurations, where the buildup/relaxation process is initiated by a single light beam, are also of great interest: The use of focused laser beams allows one to strongly extend the light-intensity range, which is practically impossible for 1D configurations. Furthermore, the high sensitivity of single-beam phase-compensating experiments allows one to measure very small ($\sim 10^{-5}$) changes of the refractive indices [4–6].

The mentioned features are indispensable for studies of weakly doped and undoped $LiNbO_3$ and $LiTaO_3$ crystals in close relation to the long-standing problem of suppression of optical damage [3,7]: First, the low light sensitivity of undoped crystals pushes researchers towards the high-intensity range. Second, a modification of the conventional one-center model leading to increasing index changes is expected in this range [8,9].

Surprisingly, kinetic processes in the 2D case remain almost uninvestigated. This hampers extraction of information about the charge-transport properties from experimental data.

Below we show, theoretically and experimentally, that the recording kinetics is not single-exponential in the 2D case within the conventional charge-transport model, including the photovoltaic effect and photoconductivity. This finding, allowing important generalizations, is of general interest. We derive also simple relations for the determination of charge transport parameters from the kinetic curves and apply them to the experiment.

We suppose that the charge transport is due to the bulk photovoltaic effect [10,11] and photoconductivity. The corresponding electric current density is

$$\vec{j} = \kappa I \vec{E} - \beta \vec{c} I, \tag{1}$$

where $I(r)$ is the light intensity, $r=(y^2+z^2)^{1/2}$ is the radial coordinate, $\vec{E}$ is the electric field, κ is the specific photoconductivity, $\vec{c}$ is the unit vector directed along the polar z axis, and β is the photovoltaic constant. The characteristic photovoltaic field is $E_{\mathrm{pv}} = \beta/\kappa$.

We present the field as $\vec{E}=-\vec{\nabla}\varphi$. The electrostatic potential φ then obeys the Poisson equation

$$(\varepsilon_\perp \partial^2/\partial y^2 + \varepsilon_\parallel \partial^2/\partial z^2)\varphi = -\rho/\varepsilon_0, \tag{2}$$

with $\varepsilon_\perp = \varepsilon_{yy}$ and $\varepsilon_\parallel = \varepsilon_{zz}$ being the transverse and longitudinal dielectric constants, respectively. The charge density ρ obeys the continuity equation

$$\partial\rho/\partial t + \vec{\nabla}\cdot\vec{j} = 0. \tag{3}$$

Equations (1)–(3) fully describe the field kinetics.

In the isotropic case, $\varepsilon_\perp = \varepsilon_\parallel = \varepsilon$, it is useful to transfer to the polar coordinates r, θ with the angle θ measured from the z axis. One can verify that $\varphi, \rho \propto \cos\theta$. Using the ansatz $\varphi = \Phi(r)\cos\theta$, $\rho = R(r)\cos\theta$ to get rid of the θ-dependence, we obtain

$$\frac{1}{r}\frac{\partial}{\partial r} r \frac{\partial \Phi}{\partial r} - \frac{\Phi}{r^2} = -\frac{R}{\varepsilon\varepsilon_0}, \tag{4}$$

$$\frac{\partial R}{\partial t} + \gamma R - \kappa I_r \frac{\partial \Phi}{\partial r} = \beta I_r, \tag{5}$$

where $\gamma(r) = \kappa I/\varepsilon\varepsilon_0$ is the dielectric-relaxation rate and $I_r = \mathrm{d}I/\mathrm{d}r$. The third term in Eq. (5) is specific for the 2D case. Without this term, the charge density ρ would change exponentially in time with the rate $\gamma(r)$.

0146-9592/09/071036-3/$15.00

The fields $E_{z,y}$ are expressed by Φ, θ, and r: $E_z=-\sin^2\theta\Phi/r-\cos^2\theta\partial\Phi/\partial r$; $E_y=\sin\theta\cos\theta(\Phi/r-\partial\Phi/\partial r)$. For $\sin\theta=0$ ($y=0$) and $\cos\theta=0$ ($z=0$), we have $E_z=-\partial\Phi/\partial r$ and $-\Phi/r$, respectively, and $E_y=0$.

Equation (4) corresponds to a standard electrostatic problem: to find the potential φ for the charge density $\rho=R(r)\cos\theta$. It is solvable by the Green function method [12]. First, we write down the solution for the surface charge localized at $r=r_0$, i.e., for $R(r)=R(r_0)\delta(r-r_0)$ with the Dirac delta function. We have $\Phi=R(r_0)r/2\varepsilon\varepsilon_0$ and $R(r_0)r_0^2/2r\varepsilon\varepsilon_0$ for $r\leqslant r_0$ and $r\geqslant r_0$, respectively. This gives a uniform field $\vec{E}=\vec{c}R(r_0)/2\varepsilon\varepsilon_0$ for $r<r_0$ and a nonuniform dipolelike field with $E_{y,z}\neq 0$ for $r>r_0$. Second, we integrate the contributions to $\Phi(r)$ from all values of r_0 to find

$$\Phi=\frac{1}{2\varepsilon\varepsilon_0}\left[\frac{1}{r}\int_0^r R(r_0)r_0^2\mathrm{d}r_0+r\int_r^\infty R(r_0)\mathrm{d}r_0\right]. \quad (6)$$

Differentiating it in r and substituting in Eq. (5), we obtain a closed integrodifferential equation for $R(r,t)$:

$$\frac{\partial R}{\partial t}+\gamma R+\frac{\gamma_r}{2}\left[\int_0^r\frac{r_0^2}{r^2}R(r_0)\mathrm{d}r_0-\int_r^\infty R(r_0)\mathrm{d}r_0\right]=q\gamma_r, \quad (7)$$

with $\gamma_r=\mathrm{d}\gamma/\mathrm{d}r$ and $q=\varepsilon\varepsilon_0E_{\mathrm{pv}}$. For the buildup process, Eq. (7) must be solved with a zero initial condition for R. As soon as $R(r,t)$ is determined, we can find $\Phi(r,t)$ from Eq. (6) and then $E_{y,z}(r,\theta,t)$. In particular, we have $E_z(0,t)=-\int_0^\infty R(r,t)\mathrm{d}r/2\varepsilon\varepsilon_0$ at the beam center.

The integral terms in Eq. (7) indicate that the charge density at point r is coupled to that at all other points. Consequently, we have a continuous spectrum of relaxation times for each r. The buildup process must be *nonexponential* in this case.

Two features of Eq. (7) are important: (i) We have $R(0,t)=0$, i.e., the charge density stays zero at the beam center. (ii) In the short-time limit, $t\ll t_d$, it gives $E_z(0,t)=E_{\mathrm{pv}}t/2t_d$, where $t_d=1/\gamma(0)$. A twofold decrease of the initial slope of $E_z(0,t)$ thus occurs in the isotropic 2D case.

Equation (7) can be solved numerically for any intensity profile. Figure 1 shows the y,z dependence of the field component E_z, which is the strongest and most important for applications, for a Gaussian beam, $I=I_0\exp(-r^2/a^2)$, and four recording times.

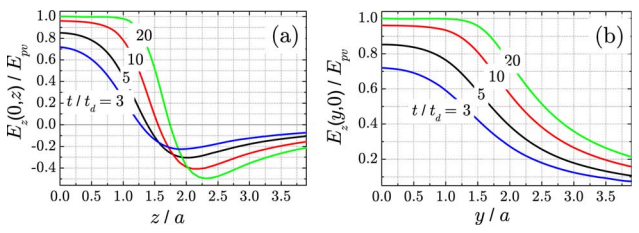

Fig. 1. (Color online) Dependences $E_z(0,z)/E_{\mathrm{pv}}$ (a) and $E_z(y,0)/E_{\mathrm{pv}}$ (b) in the isotropic case for $t/t_d=3$, 5, 10, and 20.

Since $E_z(y,z)$ is even in y and z, the curves represent E_z in the whole y,z plane. With increasing time, $E_z(y,z)$ approaches E_{pv} at the beam center, and then the saturation region with $E_z\approx E_{\mathrm{pv}}$ is expanding. The field distribution becomes thus flat near the center. The change of sign of $E_z(0,z)$ manifests itself in the index profile [3]. The field component $E_y(y,z)$, which is odd in y and z, is zero along the y and z axes. Its maximum absolute value occurs for $|\theta|=\pm 45°$; it is considerably ($\approx$2 times) smaller than that of E_z. The above features are consistent with the symmetry properties and expectations.

The solid lines in Fig. 2, calculated from Eq. (7), show the time dependence of E_z/E_{pv} at $r=0$ for three beam profiles (square, Gaussian, and Lorentzian) of the same maximum intensity. The initial slopes and the steady-state values are the same. However, the kinetics is single-exponential, $1-\exp(-t/2t_d)$, only for the square-shaped beam. For smooth beams, its slowing down when approaching the steady state is closely related to the flattening effect, i.e., to the progressive growth of $E_{y,z}$ at the beam periphery. The weaker the decrease of $I(r)$, the stronger the deviation from the single-exponential law and the slower the saturation of $E_z(0,t)$.

Now we consider the influence of the dielectric anisotropy, which is important, e.g., for $LiNbO_3$ and $BaTiO_3$ crystals. The buildup remains nonexponential, and the saturated value of E_z remains equal to E_{pv}. Using the known scaling procedure in the anisotropic Poisson equation [13], we calculate first the contribution $\mathrm{d}E_z(0)$ produced by a charged line placed at z,y:

$$\mathrm{d}E_z(0)=-\frac{\rho(y,z)}{2\pi\varepsilon_0\sqrt{\varepsilon_\parallel\varepsilon_\perp}}\frac{z\mathrm{d}y\mathrm{d}z}{z^2+(\varepsilon_\parallel/\varepsilon_\perp)y^2}. \quad (8)$$

In the short-time limit, we have $\rho(y,z)\approx\beta t\mathrm{d}I/\mathrm{d}z$ from Eqs. (1) and (3). Integrating Eq. (8) over y and z, we obtain for the Gaussian beam

$$\frac{E_z(0,t)}{E_{\mathrm{pv}}}=\frac{\kappa I_0 t}{\varepsilon_0(\varepsilon_\parallel+\sqrt{\varepsilon_\parallel\varepsilon_\perp})}. \quad (9)$$

For $\varepsilon_\parallel=\varepsilon_\perp=\varepsilon$ we return to the isotropic case. For

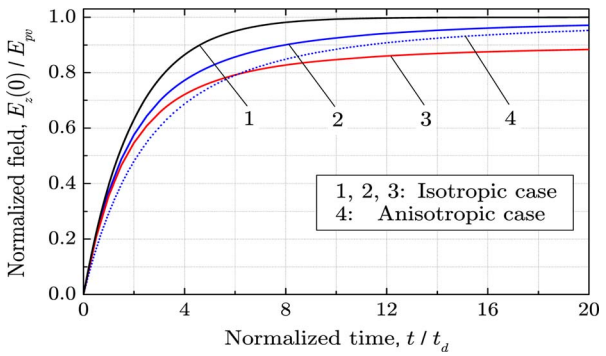

Fig. 2. (Color online) Simulated time dependences of E_z at $r=0$. Solid curves 1, 2, and 3 correspond to the square-, Gaussian-, and Lorentzian-shaped beams for $\varepsilon_\perp/\varepsilon_\parallel=1$. Curve 4 is plotted for a Gaussian-shaped beam and $\varepsilon_\perp/\varepsilon_\parallel=2.9$.

$LiNbO_3$ and $BaTiO_3$ crystals we have $\varepsilon_\perp/\varepsilon_\parallel \approx 2.9$ and 30 [3]. Correspondingly, the initial slope of $E_z(0,t)$ is $\approx$2.7 and 6.5 times smaller compared to the 1D case. Line 4 in Fig. 2 shows the whole "anisotropic" kinetic curve, calculated numerically from Eqs. (1)–(3), for $\varepsilon_\perp/\varepsilon_\parallel = 2.9$ and the Gaussian intensity profile. It is noticeably lower than the "isotropic" curve 2.

An important generalization of the above results: they can also be applied to nonphotovoltaic photoconductive media. If an external field E_0 is applied in the z direction, the necessary modification is the replacement $E_{pv} \to -E_0$.

The nonexponential kinetics is validated experimentally: a strong ordinarily (o-) polarized Gaussian light beam at 514 nm with the $1/e$ radius $a_{514} \approx 30$ μm and $I_0 = (10^1 - 8\times10^4)$ W/cm^2 is incident on the x face of an undoped 1 mm thick $LiNbO_3$ crystal. The birefringence change $\delta n = \delta(n_e - n_o)$ is monitored by the standard phase-compensation method [4,6] using a weak nonperturbing test beam at 633 nm with $a_{633} = 15$ μm propagating coaxially to the recording beam. This change is $\delta n = (n_e^3 r_{33} - n_o^3 r_{13}) E_z/2$, where $n_{o,e}$ are the initial refractive indices for the o,e waves and r_{33} and r_{13} are the known electro-optic constants. By measuring $\delta n(t)$, which can be resolved of the order of 10^{-5}, we calculate $E_z(t)$ at $r = 0$.

A representative example of many measurements is shown in Fig. 3. The experimental kinetics is fast initially and slow when approaching the steady state; it is far from being single-exponential. Furthermore, it is in good agreement with the theoretical dependence calculated for the Gaussian beam profile and $\varepsilon_\perp/\varepsilon_\parallel = 2.9$.

The saturated value of $E_z(0,t)$ gives the photovoltaic field $E_{pv} \approx 6.8$ kV/cm, with Eq. (9) the initial slope corresponds to the specific photoconductivity $\kappa \approx 3.9\times10^{-16}$ cm/V^2, and the product κE_{pv} gives the photovoltaic coefficient $\beta \approx 2.6\times10^{-12}$ A/W. The estimated value of E_{pv} is about one order of magnitude smaller than that typical of $LiNbO_3$:Fe crystals. It remains roughly the same for $I_0 \ll 10^3$ W/cm^2.

The photovoltaic field admits a general estimate $E_{pv} = l_{pv}/\mu\tau$, where $l_{pv} = (0.5-1)$ Å is an average polar displacement of a photoexcited electron per absorbed photon and $\mu\tau$ is the mobility–lifetime product of photoexcited carriers, characterizing the photoconductivity [10,11]. Since the value of l_{pv}, in contrast to that of $\mu\tau$, varies slightly in doped $LiNbO_3$ and $LiTaO_3$ crystals, the most probable reason for the decrease of E_{pv} in undoped samples is an increase of the $\mu\tau$ product. Unfortunately, the values of l_{pv} and $\mu\tau$ cannot be measured directly here because of nonmeasurable light absorption.

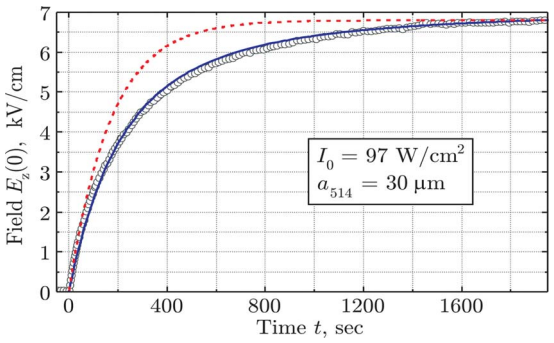

Fig. 3. (Color online) Measured (dots) and simulated (solid curve) dependences $E_z(t)$. The dashed curve is a single-exponential fit.

With the common cw light sources, our method is applicable up to $I_0 \approx 10^5$ W/cm^2. For $I_0 \gtrsim 10^3$ W/cm^2, we have found a considerable (about one order of magnitude) increase of E_{pv} in undoped $LiNbO_3$ crystals. Qualitatively, this feature is in line with literature data [3,6,8]. Systematic studies of the photoelectric parameters are beyond the scope of this Letter.

In conclusion, we have shown that the buildup process of the space-charge field under light in photorefractive crystals is far from a single-exponential one in the 2D case. The particular form of kinetic curves is strongly affected by the shape of the intensity profile, and detection of nonexponential kinetics does not indicate complicated recording mechanisms. Two measurable characteristics—the saturated value of the birefringence change $\delta n(t)$ at the beam center and the initial slope of $\delta n(t)$—are sufficient to determine the main photoelectric parameters. The necessary relations account for specific 2D effects and the influence of the dielectric anisotropy. The data obtained form a basis for the studies of photoelectric properties of undoped $LiNbO_3$ and $LiTaO_3$ crystals in a wide intensity range, which is important within the problem of suppression of optical damage.

We thank C. Becher for his experimental support. Financial support from the Deutsche Forschungsgemeinschaft (German Research Foundation) and the Deutsche Telekom AG is gratefully acknowledged.

References

1. N. V. Kukhtarev, Sov. Tech. Phys. Lett. **2**, 438 (1976).
2. L. Solymar, D. Webb, and A. Grunnet-Jepsen, *The Physics and Applications of Photorefractive Materials* (Clarendon, 1996), Chap. 5.
3. *Photorefractive Materials and Their Applications II*, P. Günter and J.-P. Huignard, eds. (Springer, 2007), Chaps. 3, 4, and 6.
4. A. Yariv and P. Yeh, *Optical Waves in Crystals* (Wiley Interscience, 2003), pp. 241–243.
5. F. S. Chen, J. Appl. Phys. **40**, 3389 (1969).
6. F. Jermann, M. Simon, and E. Krätzig, J. Opt. Soc. Am. B **12**, 2066 (1995).
7. A. Ashkin, G. D. Boyd, J. M. Dziedzic, R. G. Smith, A. A. Ballman, J. J. Levinstein, and K. Nassau, Appl. Phys. Lett. **9**, 72 (1966).
8. F. Jermann and J. Otten, J. Opt. Soc. Am. B **10**, 2085 (1993).
9. M. Carrascosa, J. Villarroel, J. Carnicero, A. Garcia-Cabanes, and J. M. Cabrera, Opt. Express **16**, 115 (2008).
10. A. M. Glass, D. von der Linde, and T. J. Negran, Appl. Phys. Lett. **25**, 233 (1974).
11. V. Fridkin and B. Sturman, *The Photovoltaic and Photorefractive Effects in Noncentrosymmetric Materials* (Gordon & Breach, 1992).
12. J. D. Jackson, *Classical Electrodynamics* (Wiley, 1998).
13. L. D. Landau and E. M. Lifshitz, *Electrodynamics of Continuous Media* (Pergamon, 1960), pp. 61–62.